Synthesis of Co_3O_4 nanoparticles with block and sphere morphology, and investigation into the influence of morphology on biological toxicity

VENKATARAMANAN RAMAN[1], SHRUTHI SURESH[1], PHILIP ANTHONY SAVARIMUTHU[2], THIAGARAJAN RAMAN[1,3], ARISTIDES MICHAEL TSATSAKIS[4,5], KIRIL SERGEEVICH GOLOKHVAST[5] and VINOD KUMAR VADIVEL[2]

Departments of [1]Bioengineering, [2]Chemistry and [3]Centre for Research on Infectious Diseases, School of Chemical & Biotechnology, SASTRA University, Thanjavur 613401, India; [4]Department of Forensic Sciences and Toxicology, Medical School, University of Crete, Heraklion 71003, Greece; [5]Scientific Educational Center of Nanotechnology, Far Eastern Federal University, Vladivostok 690990, Russian Federation

Received September 26, 2015; Accepted November 11, 2015

DOI: 10.3892/etm.2015.2946

Abstract. In the present study, cobalt oxide (Co_3O_4) magnetic nanoparticles with block and sphere morphologies were synthesized using various surfactants, and the toxicity of the particles was analyzed by monitoring biomarkers of nanoparticle toxicity in zebrafish. The use of tartarate as a surfactant produced highly crystalline blocks of Co_3O_4 nanoparticles with pores on the sides, whereas citrate lead to the formation of nanoparticles with a spherical morphology. Co_3O_4 structure, crystallinity, size and morphology were studied using X-ray diffractogram and field emission scanning electron microscopy. Following an increase in nanoparticle concentration from 1 to 200 ppm, there was a corresponding increase in nitric oxide (NO) generation, induced by both types of nanoparticles [Co_3O_4-NP-B (block), r=0.953; Co_3O_4-NP-S (sphere), r=1.140]. Comparative analyses indicated that both types of nanoparticle produced significant stimulation at ≥5 ppm ($P<0.05$) compared with a control. Upon analyzing the effect of nanoparticle morphology on NO generation, it was observed that Co_3O_4-NP-S was more effective compared with Co_3O_4-NP-B (5 and 100 ppm, $P<0.05$; 200 ppm, $P<0.01$). Exposure to both types of nanoparticles produced reduction in liver glutathione (GSH) activity with corresponding increase in dose (Co_3O_4-NP-B, r=-0.359; Co_3O_4-NP-S, r=-0.429). However, subsequent analyses indicated that Co_3O_4-NP-B was more potent in inhibiting liver GSH activity compared with Co_3O_4-NP-S. Co_3O_4-NP-B proved to be toxic at 5 ppm ($P<0.05$) and GSH activity was almost completely inhibited at 200 ppm. A similar toxicity was observed with both types of Co_3O_4-NPs against brain levels of acetylcholinesterase (AChE; Co_3O_4-NP-B, r=-0.180; Co_3O_4-NP-S, r=-0.230), indicating the ability of synthesized Co_3O_4-NPs to cross the blood-brain barrier and produce neuronal toxicity. Co_3O_4-NP-B showed increased inhibition of brain AChE activity compared with Co_3O_4-NP-S (1,5, and 10 ppm, $P<0.05$; 50, 100 and 200 ppm, $P<0.01$). These results suggested that the morphology of nanoparticle and surface area contribute to toxicity, which may have implications for their biological application.

Correspondence to: Dr Thiagarajan Raman, Department of Bioengineering, School of Chemical & Biotechnology, SASTRA University, Thanjavur 613401, India
E-mail: raman@biotech.sastra.edu

Dr Philip Anthony Savarimuthu, Department of Chemistry, School of Chemical & Biotechnology, SASTRA University, Thanjavur 613401, India
E-mail: philip@biotech.sastra.edu

Key words: cobalt nanoparticles, oxidative stress, morphology, toxicology, zebrafish, nanotoxicology

Introduction

Cobalt oxide (Co_3O_4) is an anti-ferromagnetic p-type semiconductor (with direct optical band gaps at 1.48 and 2.19 eV), which is considered to be among the most promising functional materials as it has gas-sensing, catalytic and electrochemical properties. Co_3O_4 has therefore been widely investigated for its potential application in solid state sensors, electrochromic devices and heterogeneous catalysts, as well as in lithium batteries (1-3). Nanostructured Co_3O_4 materials were demonstrated to have magnetic, optical, field emission and electrochemical properties that are used in various devices (2,4-7). Notably, the shape and size-dependent properties of inorganic nanomaterials have been the subject of numerous investigations, with the aim of synthesizing Co_3O_4 nanomaterials with controlled size and shape (8-10). Several techniques have been reported for the synthesis of Co_3O_4 nanostructures with different morphologies, including the nano-casting method for producing Co_3O_4 nanowires (11), the surfactant-based template approach for constructing Co_3O_4 nanoboxes (12), the mechano-chemical reaction method for the synthesis of Co_3O_4 nanoparticles (13), and the thermal

decomposition and oxidation method for the growth of Co_3O_4 nanorods (14). Cobalt nanowires are converted to Co_3O_4 nanotubes by calcination at 600˚C in air for an extended period of time (15), followed by heating of a cobalt foil for 12 h in air at 350˚C which leads to the growth of Co_3O_4 nanowalls (16). This nanostructured Co_3O_4 has been investigated for a range of shape and size-dependent properties.

The size reduction of inorganic materials into the nanoscale facilitates numerous properties and technological applications; however, the increase of surface area and reduction in density of the nanoparticles poses a risk to the human body and ecological environment compared with bulk materials. Cobalt exposure occurs from industrial use, exposure from the environment, and due to medical implants, and such exposure has been reported to result in lung fibrosis and asthma (17-21). In addition, cobalt is a known carcinogenic in animals (17,19,22). However, the toxicity of cobalt nanoparticles is not well understood. Furthermore, cobalt toxicity is complicated by the fact that unlike other metals, the biological toxicity of cobalt nanoparticles is not caused primarily by the cobalt ions released (19). Cobalt ions and metals are toxic, and studies that examined the genotoxic potential of cobalt-based materials *in vitro* using cell culture systems have shown that cobalt nanoparticles are highly genotoxic and cytotoxic (19,23-28), and are able to readily enter cells compared with cobalt ions. In addition, these studies suggested that the genotoxic potential of cobalt nanoparticles is contributed primarily by its ability to generate/induce reactive oxygen species (ROS). Cobalt-chrome nanoparticles have also been demonstrated to trigger pro-inflammatory changes, including the secretion of tumor necrosis factor-α (29). Co_3O_4 nanoparticles (Co_3O_4-NPs) have been shown to readily enter cells and trigger ROS generation (30). Similarly, tungsten carbide-cobalt nanoparticles are also genotoxic (31), inducing pro-inflammatory changes including nuclear factor-κB and activator protein-1 activation (32) and stimulating stress signaling pathways such as mitogen-activated protein kinase. In addition, cobalt-ferrite nanoparticles have been demonstrated to possess genotoxic potential, as demonstrated by its interaction with nucleic acids (33). It should be noted that the majority of toxicity studies on cobalt-based nanoparticles have been conducted using cell culture, and only recently have investigations focused on biological toxicity *in vivo*. A previous report on the toxicity of Co_3O_4-NPs demonstrated that the compound was cytotoxic, as determined by lactate dehydrogenase and acid phosphatase release in microalgae and isolated cells from bivalve gills (34). Phytoxicity of Co_3O_4-NPs has also been demonstrated in *Allium cepa* (35). These studies suggest that Co_3O_4-NP is equally toxic against plants and animals. A report by Falfushynska *et al* (36) examined the *in vivo* toxicity of cobalt from nanoscale composites in the fish species *Carassius auratus*. Hepatic toxicity of cobalt was demonstrated with metallothionein induction and apoptosis (36). Therefore, more in depth *in vivo* studies are required to elucidate the mechanism underlying the toxicity and biological responses to Co_3O_4-NPs. It should be noted that toxicity of nanoparticles is influenced by the shape (morphology), size, and surface characteristics of the particle, in addition to their interactions with one another and other molecules *in vivo* (37). This may be important in terms of the application of nanoparticles in biological systems. With regards to cobalt-based nanomaterials, the characteristics that are able to influence their toxicity have yet to be elucidated. Therefore, the present study aimed to investigate the influence of Co_3O_4-NPs morphology on its toxicity using a zebrafish model.

Co_3O_4 nanoparticles with block and sphere morphology were synthesized by changing the surfactants, and the effect of morphology on toxicity in zebrafish was examined by monitoring the biomarkers of the nanoparticles. The synthesized nanoparticle structure, size and morphologies were verified by powder X-ray diffraction pattern (PXRD) and field emission scanning electron microscopy (FE-SEM). The use of tartarate as a structure-controlling agent produced Co_3O_4 nanoparticles with block morphology (200 nm to 1 μm), whereas the use of citrate produce spherical morphology (40-60 nm). Toxicity studies revealed that Co_3O_4 morphology influences the toxicity of the nanoparticles, with spherical Co_3O_4 nanoparticles eliciting higher levels of nitric oxide (NO) in the liver, and Co_3O_4 nanoparticles with block or plate morphology eliciting increased inhibitory effects on the liver, and reducing glutathione and brain acetylcholinesterase activity. These results suggested that nanoparticle morphology, which often exhibits different material properties, also exhibits various toxicity levels, and this could have important implications for their biological applications.

Materials and methods

Chemicals. Cobalt chloride ($CoCl_2.6H_2O$), sodium tartarate, and trisodium citrate were obtained from Sun Pharmaceutical Industry, Ltd. (Mumbai, India). 2-Nitrobenzoic acid (DTNB), acetylcholine iodide, epinephrine, napthylethylenediamine dihydrochloride, and sulphanilamide were purchased from Sigma-Aldrich (St. Louis, MO, USA). All other chemicals and reagents were of the highest analytical grade and commercially available.

Preparation of Co_3O_4-NP block (Co_3O_4-NP-B) and sphere (Co_3O_4-NP-S) nanoparticles. In a typical experiment, 1.2 g $CoCl_2{\cdot}6H_2O$ was dissolved in 10 ml distilled water to form a 0.005 M solution. Organic structure-directing agent, trisodium citrate (2.94 g, 0.01 M) was separately dissolved in 10 ml distilled water. The solutions were mixed together and vigorously agitated at room temperature for 6 h. The formed precipitate was separated by centrifuging the solution at 1,872 x g for 2 min. The product was washed with distilled water and dried under vacuum (Rex RX-1S; SKU Vacuum Pump). Finally, 1.5 g dried powder was calcined at 580-600˚C in a high-temperature muffle furnace (#05; ThermalTech Engineering, Inc., Chennai, India) in air for 2 h, and stored in the furnace until cooled to room temperature. The second sample was prepared by following a similar protocol, but using sodium tartarate (0.01 M) as the organic structure-directing agent instead of sodium citrate.

Nanoparticle characterization. Co_3O_4 morphology and sizes were analyzed using FE-SEM (model JSM-6701F; JEOL Ltd., Tokyo, Japan) with a 30 kV accelerating voltage and filament current of 20 mA for 45 sec. The samples adhered onto a double-face conducting carbon tape mounted on a brass stub.

The samples were then coated with platinum which was sputtered at a current of 20 mA for 45 sec. Powder X-ray diffraction measurements were conducted using a Bruker diffractometer (XRD-Bruker D8 Advance XRD; Brucker Co., Billerica, MA, USA) with Cu Kα radiation.

Animal acclimatization. A total of 60 adult zebrafish (*Danio rerio*) irrespective of gender (length, 4-5 cm; weight, ~300 mg), were purchased from Angel Aquarium (Thanjavur, India). The fish were fed *ad libitum*, tanks cleaned and sterilized, and water replaced periodically. Water quality was monitored regularly, and its temperature was maintained at 25±2˚C. The fish were allowed to acclimatize for one week prior to nanoparticle exposure. The fish were randomly assigned to seven groups: Control group, and groups exposed to Co_3O_4-NPs at 1, 5, 10, 50, 100 and 200 ppm concentrations, with six fish in each group (200 ml/tank). All fish studies were conducted in accordance with the institutional animal ethics committee recommendations of SASTRA University (Thanjavur, India).

Co_3O_4 exposure. Co_3O_4-NPs (1, 5, 10, 50, 100 and 200 ppm for Co_3O_4-NP-B and Co3O4-NP-S morphologies, respectively) were prepared in tap water and sonicated prior to addition to the exposure tanks, using an Oscar Ultrasonics Pvt. Ltd. device. Six fish were used for each concentration and the exposure period was 15 days. The exposure was replicated twice with six fish/group. All assays were performed in duplicate. Water and Co_3O_4 nanoparticles were renewed every day. The water parameters were the following: Dissolved oxygen, 8.5±1.3 mg/l; pH, 7.58; total hardness ($CaCO_3$), 145±8.5 mg/l; chlorides, 73±3 mg/l; calcium, 4.3±0.7 mg/l; magnesium, 2.5±0.4 mg/l; alkalinity, 352±9.6 mg/l; total dissolved solids, 250±5 mg/l; and temperature, 25±2˚C.

Tissue sample preparation. Following exposure (15 days), the fish were anesthetized with 150 mM tricaine mesylate (Sigma-Aldrich) and euthanized by decapitation. The skin was removed and the liver or brain tissue samples from two fish of the same group were homogenized in ice-cold buffer (Tris-HCl, 0.1 M, pH 7.4). The tissue samples were then centrifuged (10,000 x g, 10 min, 4˚C) and the supernatant was collected and used for analyses. The brain tissue samples were also homogenized for acetylcholinesterase (AChE) assay. All assays were performed in duplicate.

Estimation of NO. NO was measured spectrophotometrically as previously described (38), using an Evolution 201 spectrophotometer (Thermo Fisher Scientific, Inc., Waltham, MA, USA). A total of 200 µl liver homogenate was mixed with Tris-HCl (pH 7.4) to form 300 µl. To this, 100 µl 0.1% napthylethylenediamine dihydrochloride and 100 µl 1% sulfanilamide were added. The solution was incubated for 10 min at room temperature prior to centrifugation (12,000 x g, 15 min, 4˚C). Optical density of the samples was measured at 540 nm against a blank containing buffer instead of the homogenate. The activity levels were expressed as µM nitrite.

Estimation of reduced glutathione (GSH). GSH levels were analyzed as previously described (39). A total of 750 µl liver homogenate was mixed with 0.5 ml 10% trichloroacetic acid and centrifuged (11,000 x g, 15 min, 4˚C). The protein-free supernatant was added to 250 µl 0.2 M disodium phosphate (pH 8.0) and 1 ml 0.6 mM DTNB (Qualigens Fine Chemicals; Thermo Fisher Scientific, Inc., Prabhadevi, India). The absorbance of the resulting yellow colored solution was read spectrophotometrically at 412 nm. GSH was expressed as µM/g weight.

AChE assay. AChE activity levels were measured using the Edmann's degradation method (40). Briefly, 100 µl brain homogenate was added to 800 µl 100 mM sodium phosphate buffer (pH 7.5). To this mixture 50 µl 10 mM DTNB solution was added and the enzymatic reaction was initiated by adding 50 µl 12.5 mM acetylthiocholine iodide. The samples were incubated at room temperature for 5 min until the development of a yellow color. Optical density of the samples was then measured at 400 nm against a blank containing buffer instead of sample. The activity levels were expressed as µM acetylthiocholine hydrolyzed/min.

Protein estimation. Protein was estimated using the method described by Lowry *et al* (41).

Statistical analyses. All assays were performed in duplicates. Results were expressed as the mean ± standard deviation of a minimum of six experiments. All exposure experiments were replicated twice with six fish in each group. The effects of an increase in nanoparticle dose on biochemical parameters was analyzed using Pearson's coefficient of correlation. One-way analysis of variance was followed by Tukey's post-hoc test to evaluate the significant difference between the control and Co_3O_4-NPs-treated fish belonging to the same group. Significant differences between the mean of the two types of Co3O4-NPs (Co_3O_4-NP-B and Co_3O_4-NP- S) were analyzed using a two-tailed Student's *t*-test. $P<0.05$ was considered to indicate a statistically significant result.

Results and Discussion

Co_3O_4 nanoparticle synthesis and characterization. Two organic structure-directing agents (sodium tartarate and trisodium citrate) were used to synthesize Co_3O_4 nanoparticles with different morphologies. The calcinations of the cobalt-tartarate complex produced block morphologies of Co_3O_4, whereas those of cobalt-citrate complexes produced nanospheres. The change in morphologies may be due to the varying coordination of organic structure-directing ligands. Cobalt with citrate ligands form water-soluble coordination complexes and display varied coordination modes depending on the conditions (42). Conversely, the addition of tartarate immediately produces water insoluble precipitates (43). The coordination differences of organic ligands have previously been used to modulate the morphologies of nanoparticles (44). The crystal structures of the products were verified by PXRD. Fig. 1 shows the PXRD pattern of Co_3O_4-NP-B and Co_3O_4-NP-S. The diffraction peaks typical of face-centered cubic Co_3O_4 are evident, and are concordant with those of standard Co_3O_4 cubic structures (JCPDS card no. 42-1467) (45). The absence of impurity peaks indicated the formation of pure Co_3O_4. The marked intense

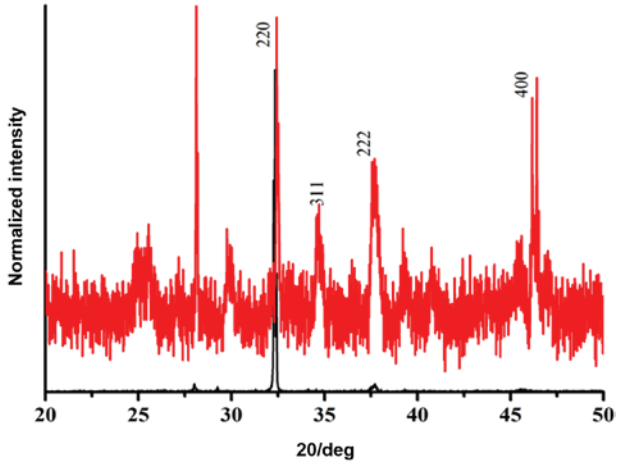

Figure 1. Powder X-ray diffraction patterns of Co_3O_4 nanoparticles synthesized using tartarate (black) and citrate (red).

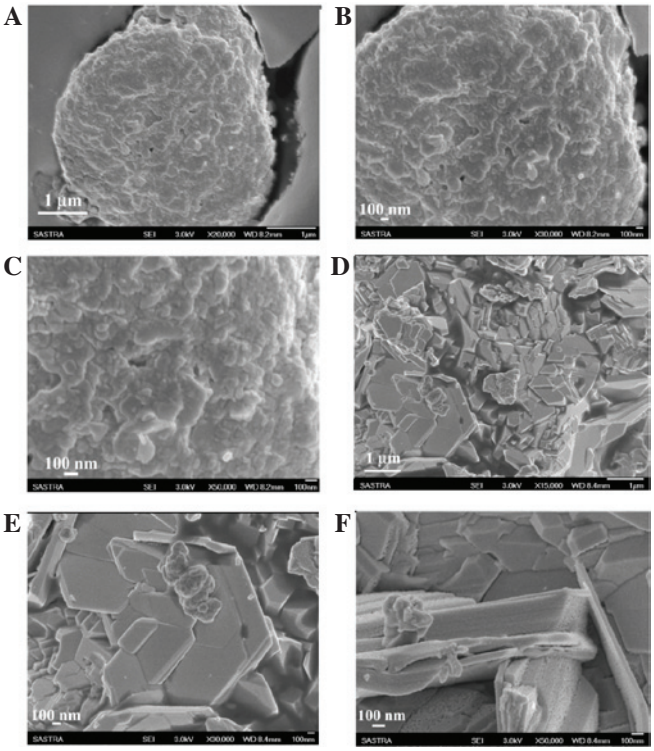

Figure 2. Field emission scanning electron microscopy image of Co_3O_4 nanoparticles synthesized using trisodium citrate (spherical morphology) at (A) x20,000 (B) x30,000 and (C) x50,000 and sodium tartarate (block morphology) at (D) x15,000, (E) x30,000 and (F) x50,000 magnification.

single PXRD peak at 220 planes for Co_3O_4-NP-B indicated adequate crystallinity of the sample with flat morphology. The PXRD of Co_3O_4-NP-S also determined the crystallinity, although this was decreased compared with Co_3O_4-NP-B, and the increased number of peaks was due to the various crystallographic faces present in sphere morphologies. Fig. 2 shows the FE-SEM images of the Co_3O_4 products Co_3O_4-NP-s and Co_3O_4-NP-B synthesized by the calcination of citrate (Fig. 2A-C) and tartarate (Fig. 2D-F) cobalt complexes, respectively. Co_3O_4-NP-S showed the presence of aggregated spherical nanostructures. The high magnification image shows the aggregation of many smaller spheres (40-60 nm) (Fig. 2C). Co_3O_4-NP-B exhibits clear blocks with 100-200 nm thickness and a length of ≥1 μm. The high magnification image shows small pores on the sides of the blocks (Fig. 2F).

Morphology-dependent toxicity of Co_3O_4-NPs. The present study aimed to examine the effects of Co_3O_4-NP morphology on its toxicity using a zebrafish model. Two forms of Co_3O_4-NPs were successfully synthesized and characterized; one with block morphology (Co_3O_4-NP-B) and the other with spherical morphology (Co_3O_4-NP-S).

Although cobalt may be present in low quantities in freshwater, cobalt concentrations can be high in water bodies near ore and coal mining sites, as well as near textile industries (46). Furthermore, environment agencies such as Environment Canada and the United Nations Environment Programme (UNEP), in addition to the Inter-Organization Programme for the Sound Management of Chemicals, have primarily examined cobalt and inorganic cobalt compounds (www.inchem.org/documents/cicads/cicads/cicad69.htm#10.2). The report by Environment Canada presented the long-term toxicity of cobalt in 15 species with values ranging from 2.9-59,000 μg/l (http://www.ec.gc.ca/ese-ees/default.asp?lang=En&n=92F47C5D-1#a7).

The data compiled by Environment Canada also demonstrated that invertebrates are more sensitive to cobalt than fishes. The most sensitive fish was shown to be the zebrafish. The data obtained from the Concise International Chemical Assessment Documents compiled by the International Programme on Chemical Safety of UNEP shows that in the

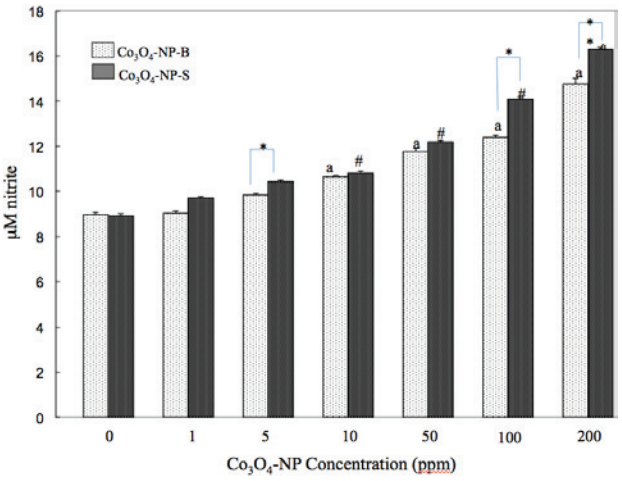

Figure 3. Effect of Co_3O_4-NP morphology on nitric oxide generation in the liver of zebrafish. Results are expressed as the mean ± standard deviation of a minimum of six determinations. All exposure experiments were replicated twice with six fish in each group. [a]The level of significance between the control and Co_3O_4-NP-B treated groups at each concentration. [#]P<0.05, control vs. Co_3O_4-NP-S treated groups at each concentration. [*]P<0.05 and [**]P<0.01 between the two types of nanoparticles for that concentration. Co_3O_4-NP-B: y=0.0267x + 9.66; r=0.9531. Co_3O_4-NP-S: y=0.0399x + 9.997; r=1.140. Co_3O_4-NP-B, block cobalt oxide nanoparticles; Co_3O_4-NP-B, spherical cobalt oxide nanoparticles.

case of water bodies close to mining and agricultural areas, cobalt concentrations may range from 1-625,000 μg/l. In addition, cobalt concentrations in polluted lake and river sediment are similar to those in the soil, and cobalt concentration levels are higher in suspended sediment compared with

bottom sediment (47). This may be due to the finer size of the suspended particles. This property could also influence exposure patterns and subsequent bioaccumulation in aquatic organisms. It should be noted that until recently few studies have been conducted on the particle size or morphology of cobalt in toxicity evaluations. However, recent studies on cobalt nanoparticles used 0.0001-1 mg/l in the sperm cells of sea urchins (48,49) and 1-40 μg/ml in human respiratory cells (50). The high concentrations of cobalt nanoparticles in polluted aquatic systems and the lack of reliable data on dosage led to the examination of 1-200 ppm Co_3O_4 nanoparticles in the present study. Furthermore, to derive baseline data on the influence of morphology on toxicity, two types of Co_3O_4 nanoparticles were compared at the same concentrations.

In the present study, the toxicity profile of the two types of Co_3O_4-NPs were evaluated by analyzing three biomarkers of nanoparticle toxicity; NO, GSH and AChE. As shown in Fig. 3, Co_3O_4-NP-B and Co_3O_4-NP-S stimulated NO generation in the liver of zebrafish, as compared with the control. NO levels increased from 1-200 ppm in a dose-dependent manner following exposure to both types of nanoparticle (Co_3O_4-NP-B, r=0.953 and Co_3O_4-NP-S, r=1.140). Both types of nanoparticle induced a significant NO level increase at ≥5 ppm (P<0.05), as compared with the control. In addition, the results demonstrated that Co_3O_4-NP-S was more effective (5-100 ppm, P<0.05; 200 ppm, P<0.01) at stimulating NO generation, as compared with nanoparticles with block morphologies (Co_3O_4-NP-B). The significant difference in NO generation induced by the two types of nanoparticles was most marked at 100 and 200 ppm. These results suggested that Co_3O_4-NPs, like other metal-based nanoparticles (51), are capable of inducing ROS production in tissues, which may lead to cellular damage. A previous study employing rodent and human cell lines have demonstrated the genotoxicity of Co_3O_4-NPs (30) and ROS has been suggested to be the predominant cause of this genotoxic potential. The study also reported that cobalt caused the rapid induction of ROS when supplied as Co_3O_4-NPs compared with cobalt ions ($CoCl_2$), and the nano form had an increased ability to enter into cells compared with the ionic form. In an *in vivo* analysis using rats, subcutaneous implantation of Co_3O_4-NPs was shown to result in nodule formation as malignant mesenchymal tumors (52). Other studies employing *in vitro* experiments have demonstrated superoxide and hydroxyl radical generation by Co-Cr nanoparticles (27). Therefore, Co_3O_4-NPs are capable of generating and/or inducing ROS that, combined with the ability of Co_3O_4-NPs to cross into cells (30), may result in widespread cellular damage.

Co_3O_4-NPs are able to enter cells and the nucleus, leading to cellular damage, as was demonstrated by analyzing GSH activity levels in the liver tissue samples of fish exposed to Co_3O_4-NPs. As shown in Fig. 4, exposure to both types of nanoparticle resulted in a reduction in liver GSH activity levels in a dose-dependent manner (Co_3O_4-NP-B, r=-0.359 and Co_3O_4-NP-S, r=-0.429). However, when the effect of morphology was analyzed, it appeared that Co_3O_4-NP-B was a more potent inhibitor of liver GSH activity compared with Co_3O_4-NP-S (1, 5 and 10 ppm, P<0.05; 100 and 200 ppm, P<0.01). Co_3O_4-NP-B was toxic at 5 ppm (P<0.05) and GSH activity was almost entirely inhibited at 200 ppm. This was

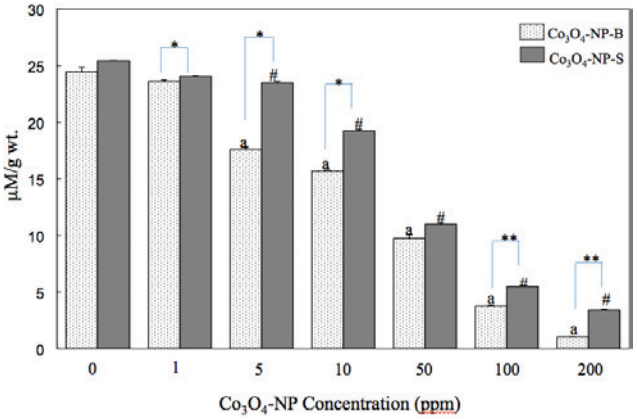

Figure 4. Effect of Co_3O_4-NP morphology on glutathione activity in the liver of zebrafish. Results are expressed as the mean ± standard deviation of a minimum of six determinations. All exposure experiments were replicated twice with six fish in each group. [a]The level of significance between the control and Co_3O_4-NP-B treated groups at each concentration. [#]P<0.05, control vs. Co_3O_4-NP-S treated groups at each concentration. [*]P<0.05 and [**]P<0.01 between the two types of nanoparticles for that concentration. Co_3O_4-NP-B: y=-0.114 x + 17.57; r=-0.3592. Co_3O_4-NP-S: y=-0.1079 x + 21.74; r=-0.4290. Co_3O_4-NP-B, block cobalt oxide nanoparticles; Co_3O_4-NP-B, spherical cobalt oxide nanoparticles.

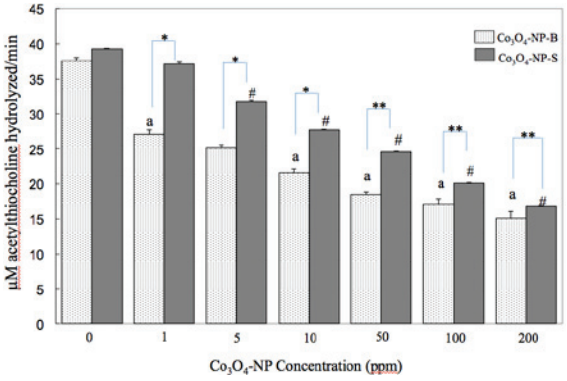

Figure 5. Effect of Co_3O_4-NP morphology on acetylcholinesterase activity in the brain of zebrafish. Results are expressed as the mean ± standard deviation of a minimum of six determinations. All exposure experiments were replicated twice with six fish in each group. [a]The level of significance between the control and Co_3O_4-NP-B treated groups at each concentration. [#]P<0.05, control vs. Co_3O_4-NP-S treated groups at each concentration. [*]P<0.05 and [**]P<0.01 between the two types of nanoparticles for that concentration. Co_3O_4-NP-B: y=0.0577x + 24.72; r=-0.1805. Co_3O_4-NP-S: y=-0.0976x + 33.31; r=-0.2308. Co_3O_4-NP-B, block cobalt oxide nanoparticles; Co_3O_4-NP-B, spherical cobalt oxide nanoparticles.

unlike the response observed with NO generation, wherein Co_3O_4-NP-S was more effective. These results suggest that the morphology and concentration of the nanoparticles may affect nanoparticle toxicity. Therefore, Co_3O_4-NP-induced oxidative stress in cells may be among the mechanisms underlying cobalt toxicity, and this may result in loss of cell function.

Similarly to the results obtained with GSH, the two types of Co_3O_4-NP proved to be toxic against brain AChE (Co_3O_4-NP-B, r=-0.180 and Co_3O_4-NP-S, r=-0.230), indicating that synthesized Co_3O_4-NPs possessed the ability to cross the blood-brain barrier and induce neuronal toxicity (Fig. 5). This inhibition of AChE could be attributed to the oxidative stress

induced by Co_3O_4-NPs. Between the two types of nanoparticle, Co_3O_4-NP-B ameliorated the inhibition of brain AChE activity, as compared with Co_3O_4-NP-S (1, 5 and 10 ppm, $P<0.05$; 50, 100 and 200 ppm, $P<0.01$).

In the present study two types of Co_3O_4-NPs were successfully synthesized, one with a block morphology (≥100 and 500 nm) and the other spherical (50-100 nm). The results of the present study demonstrated that morphology of the nanoparticle influenced its toxicity *in vivo*, as has been shown for other metal nanoparticles *in vitro* (37). Co_3O_4-NP-S was more effective at inducing NO generation in the liver, whereas Co_3O_4-NP-B was effective at inhibiting liver GSH and brain AChE activity. These differences in toxicity show that distinct mechanisms may be involved. In the case of spherical Co_3O_4-NPs, it is possible that owing to their small size they are able to easily cross the plasma membrane and accumulate inside cells, resulting in ROS generation (30). This increase in ROS generation may result in oxidative stress and cellular damage such as inhibition of GSH and AChE. Conversely, block or plate Co_3O_4-NPs were observed to be more effective at causing inhibition of liver GSH and brain AChE activity. This difference may be attributed to the fact that enzyme inhibition by nanoparticles is primarily due to adsorption (37). Although Co_3O_4-NP-S has a larger surface area when compared to Co_3O_4-NP-B, due to its smaller size and high curvature Co_3O_4-NP-S helps to preserve native protein structure and activity. For GSH, it is possible that its adsorption onto Co_3O_4-NP-B may result in its sequestration. These results are concordant with those from a previous study which demonstrated that adsorption of lysozyme onto larger sized spherical silica nanoparticles results in increased loss of α-helicity, and thus unfolding, as compared with smaller spheres (53). Similar results have been obtained for soybean peroxidase (54), subtilisin (55), ribonuclease A (56), human carbonic anhydrase (57), α-chymotrypsin (58) and AChE (59).

Increased inhibition of GSH and AChE Co_3O_4-NP-B may be a result of oxidative stress, and may also be due to loss of native structure following adsorption onto the 'flat' surface of the nanoparticle. Conversely, the ability of spherical Co_3O_4-NPs to induce higher levels of NO may be due to its ability to rapidly enter cells. However, it should be noted that these effects of nanoparticle morphology on enzyme adsorption and inactivation may not be valid for all types of enzymes and nanoparticles (60), since concentration and surface characteristics of nanoparticles may also influence their toxicity. The toxicity of nanomaterials is dependent on its final state, suggesting that nanoparticles may be modified by surface modification, ion release, and interaction with biomolecules (61). This ability of nanoparticles to undergo changes makes it difficult to determine the mode of toxicity. Nevertheless, nanoparticles are known to trigger oxidative stress in cells (62). This is also facilitated by their adverse effect on cellular antioxidants, which further increases oxidative stress. Nanoparticles such as nanosilver have been shown to interact with proteins, leading to the formation of protein corona, protein unfolding, and altered protein function (62). Therefore, it is possible to speculate that a similar modification may occur with Co_3O_4 nanoparticles and GSH, resulting in loss of GSH activity. The importance of GSH in cellular homeostasis is indicated by its role in numerous disease processes. GSH supplies reducing equivalents (63), and is therefore important for the regulation of cellular oxidative stress (64). Cellular proteins undergo irreversible modifications due to enhanced oxidative stress (65), and thus affect protein functions. Co_3O_4 nanoparticles may combine with cellular proteins and interfere with GSH activity, leading to loss of GSH activity and increase in cellular oxidative stress. This may represent one of the mechanisms underlying nanoparticle toxicity.

In conclusion, the present study demonstrated that Co_3O_4-NPs exhibit toxicity, and the morphology of Co_3O_4-NPs determined in part their toxicity. Spherical morphology induced higher levels of ROS and oxidative stress, while block or plate morphology were more effective at inhibiting enzymes, which may have important implications for their biological applications. This morphology-dependent toxicity may be due to a change in the surface area of the nanoparticles. Notably, Co_3O_4-NP-S exhibited smaller-sized spherical nanoparticles compared with micron-sized blocks of Co_3O_4-NPs-B, and therefore has a higher surface area. Furthermore, the micron-sized crystalline blocks of Co_3O_4-NPs-B settle in water, whereas Co_3O_4-NPs-S remains suspended in the water column, which increases its chances of entering into the fish. These results suggested that smaller-sized and low density nanoparticles will have higher toxicity.

This study demonstrated that morphology influences the biological toxicity of nanoparticles, with spherical Co_3O_4 nanoparticles eliciting higher levels of NO generation in the liver, and Co_3O_4 nanoparticles with block or plate morphologies exhibiting higher inhibitory effects on GSH in the liver and AchE activity in the brain. These results may have important implications for the biological roles of these nanoparticles, and for the development of strategies to inhibit the environmental toxicity of nanoparticles.

Acknowledgements

The present study was supported by a grant from the Science and Engineering Research Board of the Government of India, (grant no. SERB/F/1266/2012-13, dated 31st May 2012). This study was partially supported by the Russian Science Foundation (RSF-No 15-14-20032) which involved the participation of Dr Aristides Michael Tsatsakis and Dr Kiril Sergeevich Golokhvast.

References

1. Ando M, Kobayashi T, Iijima S and Haruta M: Optical recognition of CO and H_2 by use of gas-sensitive Au-Co_3O_4 composite films. J Mater Chem 7: 1779-1783, 1997.
2. Li WY, Xu LN and Chen J: Co_3O_4 nanomaterials in lithium-ion batteries and gas sensors. Adv Funct Mater 15: 851-857, 2005.
3. Ghosh M, Sampathkumaran EV and Rao CNR: Synthesis and magnetic properties of CoO nanoparticles. Chem Mater 17: 2348-2352, 2005.
4. Wang RM, Liu CM, Zhang HZ, Chen CP, Guo L, Xu HB and Yang SH: Porous nanotubes of Co_3O_4: Synthesis, characterization, and magnetic properties. Appl Phys Lett 85: 2080-2082, 2004.
5. Wang X, Chen XY, Gao LS, Zheng HG, Zhang Z and Qian YT: One-Dimensional arrays of Co_3O_4 nanoparticles: Synthesis, characterization, and optical and electrochemical properties. J Phys Chem B 108: 16401-16404, 2004.
6. Yang R, Wang Z, Liu J and Chen L: Nano Co_3O_4 particles embedded in porous hard carbon spherules as anode material for Li-ion batteries. Electrochem Solid-State Lett 7: A496-A499, 2004.

7. Im Y, Lee C, Vasquez RP, Bangar MA, Myung NV, Menke EJ, Penner RM and Yun M: Investigation of a single Pd nanowire for use as a hydrogen sensor. Small 2: 356-358, 2006.
8. Wang X, Zhuang J, Peng Q and Li Y: A general strategy for nanocrystal synthesis. Nature 437: 121-124, 2005.
9. Lou XWD, Archer LA and Yang Z: Hollow Micro-/Nanostructures: Synthesis and Applications. Adv Mater 20: 3987-4019, 2008.
10. Li Y, Tan B and Wu Y: Mesoporous Co3O4 nanowire arrays for lithium ion batteries with high capacity and rate capability. Nano Lett 8: 265-270, 2008.
11. García-Pacheco G, Cabañas-Moreno JG, Yee-Madeira H and Cruz-Gandarilla F: Co_3O_4 nanoparticles produced by mechano-chemical reactions. Nanotechnology 17: 2528-2535, 2006.
12. He T, Chen D, Jiao X and Wang Y: Co_3O_4 Nanoboxes: Surfactant-templated fabrication and microstructure characterization. Adv Mater 18: 1078-1082, 2006.
13. Wang ZH, Chen XY, Zhang M and Qian YT: Synthesis of Co_3O_4 nanorod bunches from a single precursor Co(CO3)0.35Cl0.20(OH)1.10. Solid State Sci 7: 13-15, 2005.
14. Salabaş EL, Rumplecker A, Kleitz F, Radu F and Schüth F: Exchange anisotropy in nanocasted Co_3O_4 nanowires. Nano Lett 6: 2977-2981, 2006.
15. Li T, Yang S, Huang L, Gu B and Du Y: A novel process from cobalt nanowire to Co_3O_4 nanotube. Nanotechnology 15: 1479-1482, 2004.
16. Yu T, Zhu YW, Xu XJ, Shen ZX, Chen P, Lim CT, Thong JTL and Sow CH: Controlled growth and field-emission properties of cobalt oxide nanowalls. Adv Mater 17: 1595-1599, 2005.
17. Bhattacharya K, Cramer H, Albrecht C, Schins R, Rahman Q, Zimmermann U and Dopp E: Vanadium pentoxide-coated ultrafine titanium dioxide particles induce cellular damage and micronucleus formation in V79 cells. J Toxicol Environ Health A 71: 976-980, 2008.
18. Lison D, Lauwerys R, Demedts M and Nemery B: Experimental research into the pathogenesis of cobalt/hard metal lung disease. Eur Respir J 9: 1024-1028, 1996.
19. Lison D, De Boeck M, Verougstraete V and Kirsch-Volders M: Update on the genotoxicity and carcinogenicity of cobalt compounds. Occup Environ Med 58: 619-625, 2001.
20. Domingo JL: Metal-induced developmental toxicity in mammals: A review. J Toxicol Environ Health 42: 123-141, 1994.
21. Magaye R, Zhao J, Bowman L and Ding M: Genotoxicity and carcinogenicity of cobalt-, nickel- and copper-based nanoparticles. Exp Ther Med 4: 551-561, 2012.
22. Kuo CY, Wong RH, Lin JY, Lai JC and Lee H: Accumulation of chromium and nickel metals in lung tumors from lung cancer patients in Taiwan. J Toxicol Environ Health A 69: 1337-1344, 2006.
23. De Boeck M, Kirsch-Volders M and Lison D: Cobalt and antimony: Genotoxicity and carcinogenicity. Mutat Res 533: 135-152, 2003.
24. Beyersmann D and Hartwig A: The genetic toxicology of cobalt. Toxicol Appl Pharmacol 115: 137-145, 1992.
25. Ponti J, Sabbioni E, Munaro B, Broggi F, Marmorato P, Franchini F, Colognato R and Rossi F: Genotoxicity and morphological transformation induced by cobalt nanoparticles and cobalt chloride: An in vitro study in Balb/3T3 mouse fibroblasts. Mutagenesis 24: 439-445, 2009.
26. Colognato R, Bonelli A, Ponti J, Farina M, Bergamaschi E, Sabbioni E and Migliore L: Comparative genotoxicity of cobalt nanoparticles and ions on human peripheral leukocytes in vitro. Mutagenesis 23: 377-382, 2008.
27. Papageorgiou I, Brown C, Schins R, Singh S, Newson R, Davis S, Fisher J, Ingham E and Case CP: The effect of nano- and micron-sized particles of cobalt-chromium alloy on human fibroblasts in vitro. Biomaterials 28: 2946-2958, 2007.
28. Wang Y, Aker WG, Hwang HM, Yedjou CG, Yu H and Tchounwou PB: A study of the mechanism of in vitro cytotoxicity of metal oxide nanoparticles using catfish primary hepatocytes and human HepG2 cells. Sci Total Environ 409: 4753-4762, 2011.
29. Guildford AL, Poletti T, Osbourne LH, Di Cerbo A, Gatti AM and Santin M: Nanoparticles of a different source induce different patterns of activation in key biochemical and cellular components of the host response. J R Soc Interface 6: 1213-1221, 2009.
30. Papis E, Rossi F, Raspanti M, Dalle-Donne I, Colombo G, Milzani A, Bernardini G and Gornati R: Engineered cobalt oxide nanoparticles readily enter cells. Toxicol Lett 189: 253-259, 2009.
31. Anard D, Kirsch-Volders M, Elhajouji A, Belpaeme K and Lison D: In vitro genotoxic effects of hard metal particles assessed by alkaline single cell gel and elution assays. Carcinogenesis 18: 177-184, 1997.
32. Ding M, Kisin ER, Zhao J, Bowman L, Lu Y, Jiang B, Leonard S, Vallyathan V, Castranova V and Murray AR: Size-dependent effects of tungsten carbide-cobalt particles on oxygen radical production and activation of cell signaling pathways in murine epidermal cells. Toxicol Appl Pharmacol 241: 260-268, 2009.
33. Pershina AG, Sazonov AE, Novikov DV, Knyazev AS, Izaak TI, Itin VI, Naiden EP, Magaeva AA and Terechova OG: Study of DNA interaction with cobalt ferrite nanoparticles. J Nanosci Nanotechnol 11: 2673-2677, 2011.
34. Rebello V, Shaikh S and Desai PV: Toxicity of cobalt oxide nanoparticles on microalgae (Navicula sp. and Chetoceros sp.) and Bivalve (Meritrix meritrix) cells. In: 2010 International Conference on Environmental Engineering and Applications. Singapore, pp195-199, 2010. http://toc.proceedings.com/09360webtoc.pdf
35. Ghodake G, Seo YD and Lee DS: Hazardous phytotoxic nature of cobalt and zinc oxide nanoparticles assessed using Allium cepa. J Hazard Mater 186: 952-955, 2011.
36. Falfushynska H, Gnatyshyna L, Turta O, Stoliar O, Mitina N, Zaichenko A and Stoika R: Responses of hepatic metallothioneins and apoptotic activity in *Carassius auratus* gibelio witness a release of cobalt and zinc from waterborne nanoscale composites. Comp Biochem Physiol C Toxicol Pharmacol 160: 66-74, 2014.
37. Wu Z, Zhang B and Yan B: Regulation of enzyme activity through interactions with nanoparticles. Int J Mol Sci 10: 4198-4209, 2009.
38. Manikandan R, Thiagarajan R, Beulaja S, Sudhandiran G and Arumugam M: Effect of curcumin on selenite-induced cataractogenesis in Wistar rat pups. Curr Eye Res 35: 122-129, 2010.
39. Manikandan R, Thiagarajan R, Beulaja S, Sudhandiran G and Arumugam M: Curcumin prevents free radical-mediated cataractogenesis through modulations in lens calcium. Free Radic Biol Med 48: 483-492, 2010.
40. Ellman GL, Courtney KD, Andres V Jr and Feather-Stone RM: A new and rapid colorimetric determination of acetylcholinesterase activity. Biochem Pharmacol 7: 88-95, 1961.
41. Lowry OH, Rosebrough NJ, Farr AL and Randall RJ: Protein measurement with the Folin phenol reagent. J Biol Chem 193: 265-275, 1951.
42. Matzapetakis M, Dakanali M, Raptopoulou CP, Tangoulis V, Terzis A, Moon N, Giapintzakis J and Salifoglou A: Synthesis, spectroscopic, and structural characterization of the first aqueous cobalt(II)-citrate complex: Toward a potentially bioavailable form of cobalt in biologically relevant fluids. J Biol Inorg Chem 5: 469-474, 2000.
43. Haines RA, Kipp EB and Reimer M: Cobalt(III) complexes containing optically active tartaric acid. Inorg Chem 13: 2473-2476, 1974.
44. Theja GS, Lowrence RC, Ravi V, Nagarajan S and Anthony SP: Synthesis of Cu2O micro/nanocrystals with tunable morphologies using coordinating ligands as structure controlling agents and antimicrobial studies. CrystEngComm 16: 9866-9872, 2014.
45. Lou XW, Deng D, Lee JY, Feng J and Archer LA: Self-supported formation of needlelike Co3O4 nanotubes and their application as lithium-ion battery electrodes. Adv Mater 20: 258-262, 2008.
46. Diamond JM, Winchester EL, Mackler DG, Rasnake WJ, Fanelli JK and Gruber D: Toxicity of cobalt to fresh-water indicator species as a function of water hardness. Aquat Toxicol 22: 163-179, 1992.
47. Gibbs RJ: Metals in the sediments along the Hudson River estuary. Environ Int 20: 507-516, 1994.
48. Gambardella C, Aluigi MG, Ferrando S, Gallus L, Ramoino P, Gatti AM, Rottigni M and Falugi C: Developmental abnormalities and changes in cholinesterase activity in sea urchin embryos and larvae from sperm exposed to engineered nanoparticles. Aquat Toxicol 130-131: 77-85, 2013.
49. Gambardella C, Ferrando S, Morgana S, Gallus L, Ramoino P, Ravera S, Bramini M, Diaspro A, Faimali M and Falugi C: Exposure of *Paracentrotus lividus* male gametes to engineered nanoparticles affects skeletal bio-mineralization processes and larval plasticity. Aquat Toxicol 158: 181-191, 2015.
50. Cavallo D, Ciervo A, Fresegna AM, Maiello R, Tassone P, Buresti G, Casciardi S, Iavicoli S and Ursini CL: Investigation on cobalt-oxide nanoparticles cyto-genotoxicity and inflammatory response in two types of respiratory cells. J Appl Toxicol 35: 1102-1113, 2015.

51. Yang H, Liu C, Yang D, Zhang H and Xi Z: Comparative study of cytotoxicity, oxidative stress and genotoxicity induced by four typical nanomaterials: The role of particle size, shape and composition. J Appl Toxicol 29: 69-78, 2009.
52. Hansen T, Clermont G, Alves A, Eloy R, Brochhausen C, Boutrand JP, Gatti AM and Kirkpatrick CJ: Biological tolerance of different materials in bulk and nanoparticulate form in a rat model: Sarcoma development by nanoparticles. J R Soc Interface 3: 767-775, 2006.
53. Vertegel AA, Siegel RW and Dordick JS: Silica nanoparticle size influences the structure and enzymatic activity of adsorbed lysozyme. Langmuir 20: 6800-6807, 2004.
54. Asuri P, Bale SS, Pangule RC, Shah DA, Kane RS and Dordick JS: Structure, function, and stability of enzymes covalently attached to single-walled carbon nanotubes. Langmuir 23: 12318-12321, 2009.
55. Asuri P, Karajanagi SS, Vertegel AA, Dordick JS and Kane RS: Enhanced stability of enzymes adsorbed onto nanoparticles. J Nanosci Nanotechnol 7: 1675-1678, 2007.
56. Shang W, Nuffer JH, Dordick JS and Siegel RW: Unfolding of ribonuclease A on silica nanoparticle surfaces. Nano Lett 7: 1991-1995, 2007.
57. Lundqvist M, Sethson I and Jonsson BH: Protein adsorption onto silica nanoparticles: Conformational changes depend on the particles' curvature and the protein stability. Langmuir 20: 10639-10647, 2004.
58. Fischer NO, 5 CM, Simard JM and Rotello VM: Inhibition of chymotrypsin through surface binding using nanoparticle-based receptors. Proc Natl Acad Sci USA 99: 5018-5023, 2002.
59. Wang Z, Zhao J, Li F, Gao D and Xing B: Adsorption and inhibition of acetylcholinesterase by different nanoparticles. Chemosphere 77: 67-73, 2009.
60. Gagner JE, Lopez MD, Dordick JS and Siegel RW: Effect of gold nanoparticle morphology on adsorbed protein structure and function. Biomaterials 32: 7241-7252, 2011.
61. Sanford J and Venkatapathy R: State of the Science Literature Review: Everything Nanosilver and More. In: Scientific, Technical, Research, Engineering, and Modeling Support Final Report. Varner K (ed). U. S. Environmental Protection Agency, Office of Research and Development, Washington, DC, pp1-197, 2010.
62. Saptarshi SR, Duschl A and Lopata AL: Interaction of nanoparticles with proteins: Relation to bio-reactivity of the nanoparticle. J Nanobiotechnology 11: 26, 2013.
63. Schafer FQ and Buettner GR: Redox environment of the cell as viewed through the redox state of the glutathione disulfide/glutathione couple. Free Radic Biol Med 30: 1191-1212, 2001.
64. Gilbert HF: Redox control of enzyme activities by thiol/disulfide exchange. Methods Enzymol 107: 330-351, 1984.
65. Klatt P and Lamas S: Regulation of protein function by S-glutathiolation in response to oxidative and nitrosative stress. Eur J Biochem 267: 4928-4944, 2000.